The interaction of new 4,9-diazapyrenium compounds with double stranded nucleic acids

Barbara Susanne Palm,[a] Ivo Piantanida,[b] Mladen Žinić *[b] and Hans-Jörg Schneider *[a]

[a] *FR Organische Chemie der Universität des Saarlandes, D 66041 Saarbrücken, Germany*
[b] *Laboratory for Supramolecular and Nucleoside Chemistry, Department of Chemistry and Biochemistry, Rudjer Bošković Institute, HR-10000 Zagreb, P.O.B. 1016, Croatia*

Received (in Cambridge, UK) 1st July 1999, Accepted 18th November 1999

Interactions of double stranded nucleic acids were studied with 4,9-diazapyrenium compounds, including monofunctional monocationic derivatives [4-methyl- (**1**) and 4-benzyl- (**2**)], monofunctional dicationic derivatives [4,9-dimethyl- with substituents H- (**3**) or Ph- (**4**) in the 5,10 positions and Me- (**5**) in the 2,7-positions], and bifunctional derivatives [4,4′-*p*- (**6**) and *m*- (**7**) xylylene bridged], which were described in the preceding paper. NMR spectra indicate intercalation for all ligands, with line width increases of up to 70 Hz. Thermal melting experiments and UV or fluorescence titrations were used to characterize affinities; these are essentially independent of the number of charges present in the ring systems, in line with negligible electrostatic binding contributions and with the corresponding affinities towards nucleotides (reported in the preceding paper). Substituents at the pyrenium rings have relatively little influence on the binding, with the exception of two phenyl groups, which lower the affinity, probably due to steric hindrance. Several melting curves are biphasic; in particular with the RNA-type polyA-polyU one observes transition points above and below the original denaturation point. Ligands containing two diazapyrenium rings bridged either by a *m*- or by a *p*-xylylene unit show distinctly higher affinities for the latter, and in Scatchard analyses a ligand to nucleotide ratio of $n = 0.08$, suggesting bisintercalation. Viscometry, however, shows a rather uniform length increase of the calf thymus DNA double helix with slopes of $a = 1.1$, similar to the known monointercalator ethidium bromide ($a = 1.0$). The monofunctional compounds exhibit some noteworthy RNA selectivity.

Introduction

Intercalation of aromatic compounds in double stranded (ds) nucleic acids is of paramount significance for many biologically and medicinally important interactions.[1] The underlying binding mechanisms have been the focus of numerous investigations with partially contradicting mechanistic conclusions,[2] but it is clear that the stacking between nucleobases and ligands increases with the size of the ligand π-surfaces. Classical intercalators such as ethidium bromide† (EB) or acridines therefore show strong affinities and are the basis of many applications in molecular biology and medicinal chemistry.[1,3] Recently Wilson *et al.*[4] have discovered that intriguing antiviral properties of EB are related to rather strong intercalation with RNA. In view of this, the strong stacking interactions of 4,9-diazapyrenium derivatives with nucleotides, and the anticancer activity discussed in the preceding paper,[5] it was of interest to study the behaviour of the same compounds towards ds nucleic acids. The new ligands can be promising candidates for the development of RNA selective binders, and also shed light on the importance of positive charges within the aromatic ligand moiety, which has been under debate.[6]

The novel dicationic 2,7-diazapyrenium ligands (Chart 1) combine the molecular features of pyrene, methylviologen and other heteroaromatic nucleic acid intercalators.[7] The intercalation of such compounds and their use for DNA cleavage by visible light and subsequent electron transfer has been demonstrated already.[7,8] The new systems studied in the preceding paper with nucleotides also comprise potential bisintercalators, and may lead to particularly efficient new systems also for photocleavage and/or phototherapy of cancer. In the present work the interaction of the new derivatives with ds nucleic acids is studied by melting analysis, by fluorescence and UV/Vis as well as by NMR spectroscopy and viscometry.

† IUPAC name for ethidium bromides is 3,8-diamino-5-ethyl-6-phenylphenanthridin-5-ium bromide.

Results

Methods

Melting experiments (see Tables 1, 4 and 5, Fig. 1) were conducted as described in the literature;[9] they usually show with intercalating agents melting point increases. The UV and fluorescence titrations (see Fig. 2) were analysed with Scatchard equation and nonlinear fitting,[10] which allows simultaneous determination of the binding constant K_s and the ratio n of bound ligand to nucleotide (see Tables 2 and 3). NMR-spectroscopic data (see Fig. 4) were evaluated in analogy to earlier papers;[11] intercalation is usually characterised by upfield shifts of the ligand stacked between the nucleobases and by substantial line width increase (see Table 6). Viscosity measurements, which were performed with an automated device, indicate intercalation by the slope of plots of helix length increases (obtained from viscosity changes) *vs.* the ligand–nucleobase ratio r (see Fig. 3).[12]

Discussion

With monofunctional pyrenium compounds (Chart 1, Table 1) there is no difference between **1**, **3** and **5** (with one, two and four methyl substituents, respectively) regarding their thermal stabilisation effect on CT-DNA (for $r = 0.3$: $\Delta T_m = 11.5\ ^\circ\mathrm{C} \pm 0.1$), although **1** carries only one charge. This leads to the conclusion that in this series the binding affinity is only due to stacking interactions, and barely to any electrostatic forces. This observation is completely in line with the nucleotide affinities to

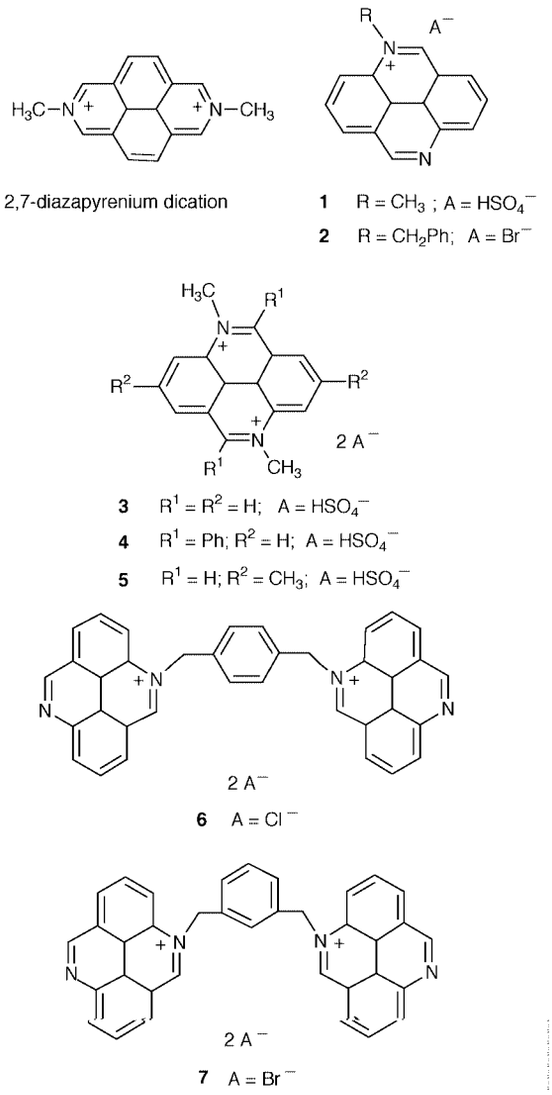

Chart 1 Overview of ligand structures **1**–**7** and the 2,7-diazapyrenium.

these compounds, which also do not depend on the number of charges present in ligand or nucleotide (see preceding article, ref. 5).

Only the monofunctional compound **4** (with two phenyl substituents) shows values for CT-DNA which are increased by 40–50% in comparison to **1**, **3**, and **5**, with for example ΔT_m = 16.1 °C for $r = 0.3$. In slight contrast, the smaller stability constant K_s of **4** with CT-DNA compared to *e.g.* **1** found by fluorescence-spectroscopy (see Tables 2 and 3) might be due to an easier insertion of the sterically hindered compound **4** in a CT-DNA-duplex which has already started unwinding at higher temperatures, rather than in CT-DNA at room temperature. Intercalators with bulky substituents, for example in the side chain, are known as "threading intercalators"; they also give smaller binding constants because of a less complete overlap with the adjacent base pairs, caused by the intercalator axis being perpendicular to the base pair long axis.[13] The two phenyl groups directly attached to the intercalation moiety of **4** should also lead to such a geometry and to a decreased constant, whereas the melting which reflects a beginning opening of the base pairs at higher temperatures could facilitate a better overlap: It could lead also to a stabilising interaction of the phenyl groups in both grooves, resulting in a higher melting point increase. However, the difference in ΔT_m and in the UV-derived K_s value between ligands **1** and **4** is not far from the experimental error, and the constants measured by UV are the same for **1** and **4** (see Table 3).

The UV and fluorescence-derived equilibrium constants K_s and the ligand/nucleotide ratios n (Table 3) with the ligands **1** and **2** bearing one charge are similar to those with EB, although somewhat lower (with EB $K = 9.5 \times 10^5$ M^{-1}, with **1** and **2** 1–2 $\times 10^5$ M^{-1}), and agree with the expected monointercalation. The doubly charged **4** shows weaker binding, which as discussed above is due to the presence of the two bulky phenyl rings. It is interesting to note that the observed order of K_s values for CT-DNA parallel those found in binding of nucleotides[5] with **4** being the weakest nucleotide binder.

Table 1 ΔT_m values (°C) of **1**, **3**, **4**, **5**, and **7** in *low* salt citric acid buffer pH = 5.0[a]

		r		
		0.1	0.2	0.3
1	CT-DNA	5.9	9.0	11.4
	PolydA-polydT	1.1	2.1	3.1
	PolyA-polyU	−2.6/+5.1	−4.4/+7.0	−6.0/+8.4
3	CT-DNA	5.9	9.2	11.6
	PolydA-polydT	0.9	1.8	2.4
	PolyA-polyU	−1.2/+3.6	−2.0/+5.2	−2.2/+6.3
4	CT-DNA	9.1	13.1	16.1
	PolydA-polydT	0.9	1.5	2.7
	PolyA-polyU	−1.6/+3.8	−2.1/+5.0	−4.0/+5.9
5	CT-DNA	5.9	9.3	11.5
	PolydA-polydT	2.0	3.2	4.1
	PolyA-polyU	−2.3/+4.6	−4.0/+6.2	−5.2/+7.4
7	CT-DNA	14.5	22.0	26.4
	PolydA-polydT	5.8[b]	13.1	17.1
	PolyA-polyU	−3.2/+6.0	−3.6/+7.3	−3.8/+7.7

[a] *r*, molar ratio of ligand/nucleic acid phosphate; CT-DNA: calf thymus DNA; ionic strength $I = 0.025$ M; error in ΔT_m: ±0.5 °C. [b] Biphasic behaviour, the second transition could not be determined.

Similarly to those with CT-DNA, the ΔT_m values for polydA-polydT for the monofunctional compounds are quite low (for $r = 0.3$ between 2.4 and 4.1 °C), compared to other classical intercalators. These show a melting point increase of polydA-polydT of 4.1 °C and more, even in a buffer of much higher ionic strength than the one used here (*e.g.* with acridine orange or methylene blue).[4] The ΔT_m values of polydA-polydT for all four monofunctional compounds are nearly the same.

The melting curves of RNA-type polymer polyA-polyU showed an unusual behaviour: addition of every ligand produced biphasic curves with one transition higher than the original denaturation point of polyA-polyU, and another one lower (see Fig. 1e). With increasing ligand to polymer ratio, these effects become much more pronounced. The melting profiles resemble those of the triple helical polyA-2polyU.[14] The first melting step would correspond to a triple helix going to double helical polyA-polyU and polyU; the second step would represent the transition of the duplex to the single strands. It has been observed that ligands such as porphyrins[15] induce the formation of a triple helix out of a mixture of single stranded polyA and polyU; it is feasible that some ligands also favour the formation of a triple helix out of the already present double helical polyA-polyU according to the equilibrium: 2polyA-polyU ⇌ polyA-2polyU + polyA. Furthermore, the intercalator ethidium bromide is known to lower the T_m of the triplex transition of polyA-2polyU[16] whereas it shows a stabilisation of the duplex polyA-polyU; the same pattern is valid for the binding of ethidium bromide to mixed AT- and GC-containing short triplex sequences.[17] In order to shed light on the question whether pyrenium compounds can induce triple helix formation, a mixing-curve[18] has been obtained by monitoring the absorbance of polyA–polyU-mixtures in various ratios at different wavelength in absence or presence of ligands

Table 2 Spectroscopic properties of **1** and **6**[a] and their complexes with calf thymus DNA, poly(dA-dT)$_2$ and poly(dG-dC)$_2$

Compound	Fluorescence $\lambda_{ex}/\lambda_{em}$		UV/Vis λ_{max}/nm (ε/dm^3 mol^{-1} cm^{-1})		
			poly(dA-dT)$_2$ complex	poly(dG-dC)$_2$ complex	CT-DNA complex
1	350/420	388 nm (10010)	389 nm (4213)[b]	389 nm (3585)[b]	393 nm (5025)[b]
6	392/430	393 nm (15400)	395 nm (10856)[c]	394 nm (10378)[c]	395 nm (10916)[c]

[a] Changes in electronic absorption spectra of compounds **1** and **6** upon titration with calf thymus DNA, poly(dA-dT)$_2$ and poly(dG-dC)$_2$ exhibit isosbestic points at 397 and 402 nm respectively, which points toward only two spectroscopically active species present (bound and free compounds). [b] Calculated values for 100% complex formed. [c] Experimentally obtained values for 100% complex (further additions of substrate did not produce any change in dye spectra).

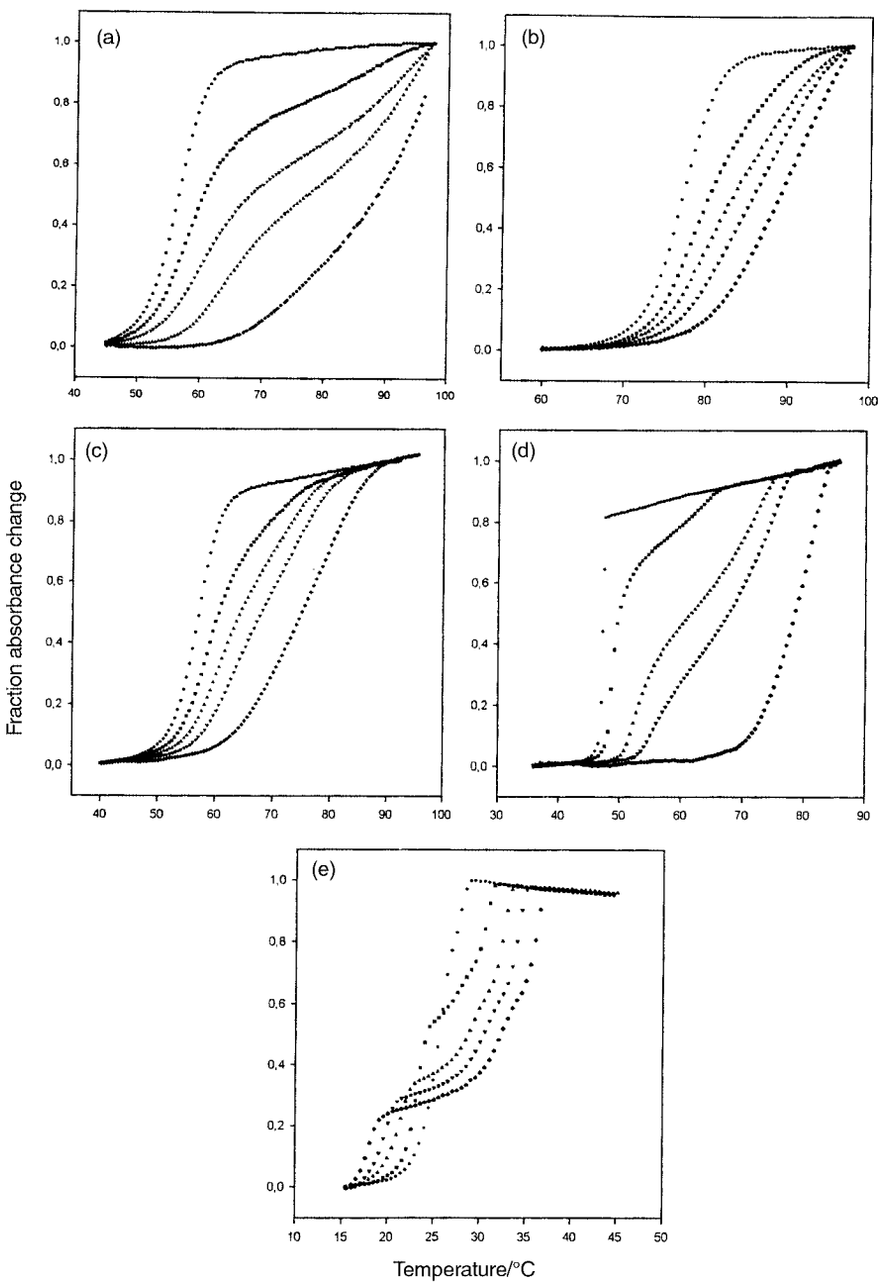

Fig. 1 Melting curves of nucleic acids with ligands. Measuring conditions see footnotes to Table 1, Table 5 and Experimental section, ligand/nucleic acid ratios indicated from left to right: (a) **6** and CT-DNA at low ionic strength, *I*; from left to right 0.0; 0.025, 0.05; 0.075; 0.125. (b) **6** and CT-DNA at high ionic strength, *I*; from left to right 0.0; 0.025; 0.05; 0.075; 0.125. (c) **7** and CT-DNA at low, *I*; from left to right 0.0; 0.025; 0.05; 0.075; 0.15. (d) **6** with polydA-polydT at low, *I*; from left to right 0.0; 0.025; 0.05; 0.1; 0.2. (e) **1** with polyA-polyU at low, *I*; from left to right 0.0; 0.1; 0.2; 0.3; 0.5.

(data not shown); this serves to establish the stoichiometries of eventually formed complexes. Afterwards, all these samples were investigated in thermal denaturation experiments (data not shown). The mixing curve showed only a straight line going from the absorbance of pure polyU to the (lower) absorbance of polyA without any inflection point. This indicates that neither a double nor a triple helix is formed. The decrease in absorbance of polyA at pH 5.0 compared to pH = 7.0, and compared to the value for polyU at both pH is attributed to the formation of a polyAH$^+$-polyAH$^+$-double helix in acidic

Table 3 Binding constants (K_s) and ratio n (bound ligand to DNA phosphate) for 4,9-diazapyrenium compounds, ethidium bromide (EB) and calf thymus DNA, poly(dA-dT)$_2$ and poly(dG-dC)$_2$ obtained from Scatchard binding isotherms[a]

	$n(10^5 K_s/M^{-1})$					
	Fluorescence			UV/Vis		
	CT-DNA	poly(dG-dC)$_2$	poly(dA-dT)$_2$	CT-DNA	poly(dG-dC)$_2$	poly(dA-dT)$_2$
EB	0.17 (9.5)	0.25 (10.2)	0.25 (11)	—	—	—
1	0.12 (1.1)	0.17 (0.7)	0.17 (0.5)	0.14 (0.5)	0.17 (0.5)	0.17 (0.3)
2	0.11 (1.8)	—	—	—[b]	—	—
4	0.16 (0.4)	—	—	0.16 (0.52)	—	—
6	0.08 (98.7)	0.23 (42)	0.16 (44)	0.15 (x[c])	0.13 (x[c])	0.17 (x[c])
7	0.14 (5.7)	—	—	—	—	—

[a] pH = 4.5, I = 0.1. [b] Too small changes in the electronic absorption spectra for accurate calculation. [c] Due to large K_s, the total ligand to DNA phosphate ratio r becomes smaller than n (bound ligand to DNA phosphate ratio) only when 80–100% complexation is reached. This prevented accurate calculation of K_s.

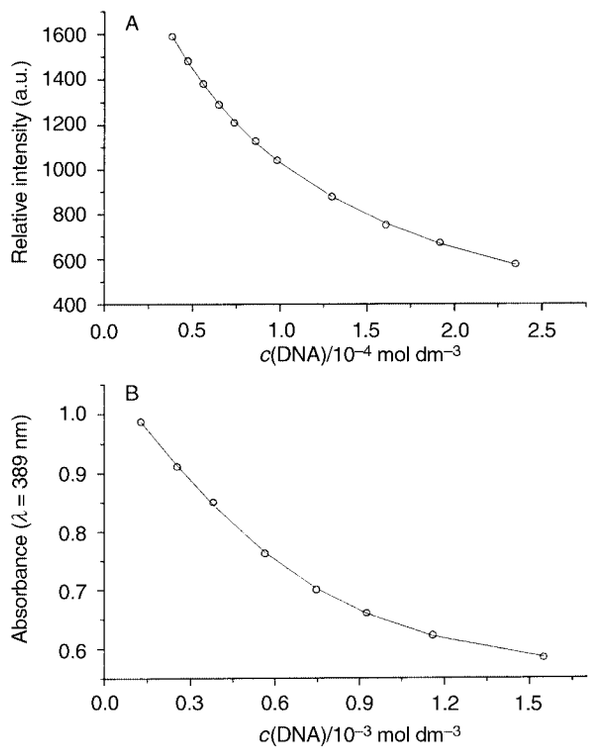

Fig. 2 Fluorimetric (A) and UV/Vis (B) titrations of **1** with CT-DNA. Experimental (○) and calculated (—) data according to Scatchard equation by nonlinear least square analysis. Measuring conditions, see footnotes to Table 3 and Experimental section.

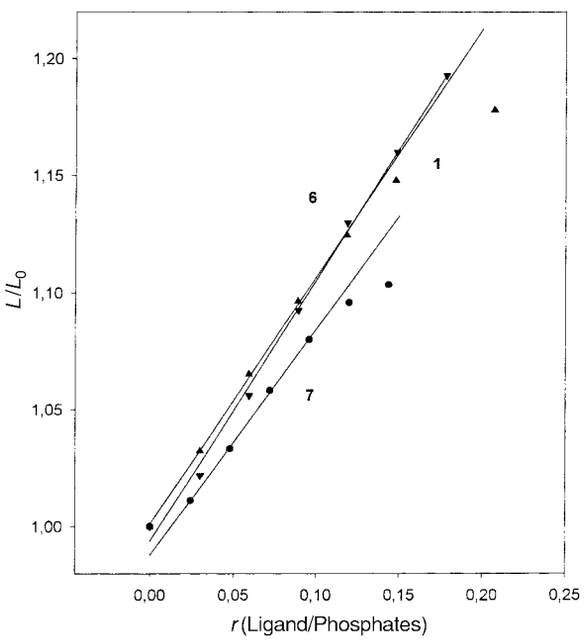

Fig. 3 Helix length extension (L/L_0) *vs.* ligand/DNA phosphate ratio plot for **1**, **6** and **7** at pH = 5.0. Measuring conditions see footnotes to Table 1 and Experimental section. Results: a = 1.1 (for **1**); 1.1 (for **6**); 1.0 (for **7**).

solutions,[19] where the adenine bases are protonated at N1. Also the melting curves of each sample (data not shown) exhibited only the melting transition of polyAH$^+$-polyAH$^+$ at about 81 °C. This stable polyAH$^+$-polyAH$^+$-complex might be the reason that a formation of polyA-polyU-duplex or polyA-2polyU or 2polyA-polyU triplexes cannot be detected: The helix displacement equilibrium polyA×B + polyC ⇌ polyA + polyB-C is shifted to the side of the more stable helix with higher melting temperature,[20] *e.g.* to polyAH$^+$-polyAH$^+$ with ~81 °C instead of polyA-polyU with ~25 °C. So neither in the mixing curve nor in the melting profiles is there evidence of triple helix formation by pyrenium ligands under these conditions. The observed biphasic behaviour of the polyA-polyU-transitions upon addition of the ligand must therefore be due to other structural features in different regions of the polymer upon ligand binding.[21]

The ΔT_m values for polyA-polyU with the monofunctional compounds lie between −2.2 and −6.0 °C for the first and between +5.9 and +8.4 °C for the second denaturation step (r = 0.3). For the same ligand, the stabilisation values for polyA-polyU are more than twice as high as those for polydA-polydT. The ratios of ΔT_m(polyA-polyU)/ΔT_m(polydA-polydT) give for all monofunctional compounds values between 1.8 (**5**) and 2.7 (**1**). This shows a selectivity for the RNA-polymer which is better than that for proflavine (r = 1.2) or acridine orange (r = 1.5) and comparable with that for ethidium bromide (r = 2.4).[4]

For the bifunctional compound **7**, with two pyrenium moieties and two positive charges, the ΔT_m values for CT-DNA are more (2 to 4 °C) than twice as high as those for the corresponding monomer **1** (Table 4), which can also be seen in the high ionic strength buffer (Table 5) and is consistent with the binding constant to CT-DNA in this buffer (five times larger than that for **1**, Tables 2 and 3). This result would speak for bisintercalation, but has also been observed with groove binders like benzimidazoles and bisbenzimidazoles binding to polydA-polydT: addition of one more charge or one more aromatic moiety can produce a dramatic enhancement of the thermal melting points.[22] Responsible for this effect is a binding contribution by hydrophobic and polar interactions at the edges of the minor groove. Groups which are capable of hydrogen bonding like hydroxy-, methoxy- and amino groups gave only a negligible contribution.[23]

Table 4 ΔT_m values (°C) of **1**, **6** and **7** in *low* salt citric acid buffer pH = 5.0[a]

		r							
		0.025	0.05	0.075	0.1	0.125	0.15	0.2	0.3
1	CT-DNA	—	3.5	—	5.9	—	7.5	9.0	11.4
	PolydA-polydT	—	0.5	—	1.1	—	1.7	2.1	3.1
	PolyA-polyU	—	−1.5/+3.8	—	−2.6/+5.1	—	−3.5/+5.9	−4.4/+7.0	−6.0/+8.4
6	CT-DNA	1.2[b]	3.3[b]	5.8[b]	10.4[b]	—	—	—	—
	PolydA-polydT	1.5[b]	4.8/23.1	8.8/27.5	11.3/28.5	20.5/31.0	31.1	34.1	37.6
	PolyA-polyU	−7.1/+8.2	−7.1/+8.7	−7.5/+8.3	−7.4/+8.4	−7.4/[d]	[c]	[c]	[c]
10% DMSO	CT-DNA	1.1[b]	2.3[b]	4.5[b]	8.6[b]	—	—	—	—
7	CT-DNA	2.0/14.8	4.3/15.9	13.0	14.5	17.1	18.7	22.0	26.4
	PolydA-polydT	2.0/5.6	2.9/6.3	5.1/10.8	≙5.8[b]	10.8	11.3	13.1	17.1
	PolyA-polyU	−1.3/+3.2	−2.0/+4.6	−2.5/+5.2	−3.2/+6.0	—	−3.5/+6.9	−3.6/+7.3	−3.8/+7.7
10% DMSO	CT-DNA	1.4/12.1	3.1/15.0	5.8/17.4	14.4	—	—	—	—

[a] See footnotes to Table 1, $I = 0.025$ M; [b] T_m derived from the first transition step. [c] No regular curves with deflection points. [d] Determination not possible.

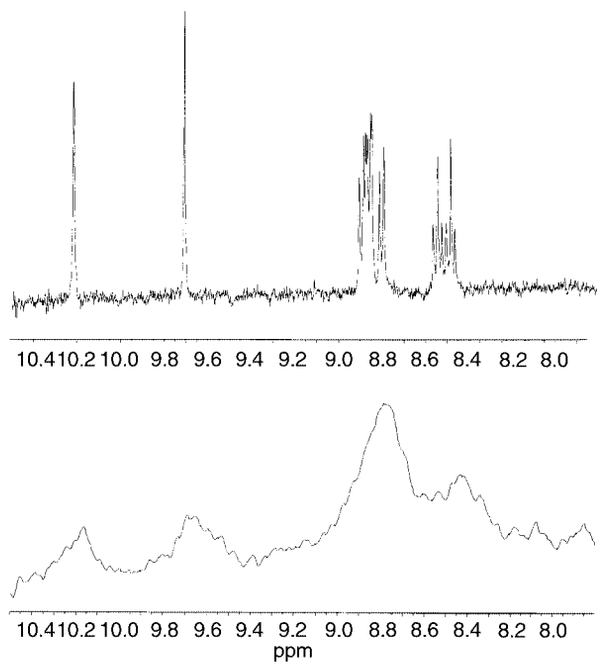

Fig. 4 NMR spectra of **1** at pH = 5.0. Measuring conditions see footnotes to Table 6 and experimental section; upper trace: without ligand; lower trace: ligand/nucleotide ratio $r = 1.7$.

The melting point increases for **7** with polydA-polydT are 5–6 times higher than for its monofunctional analogue **1** (*e.g.* $\Delta T_m = 17.1$ °C for $r = 0.3$), which could be due to a possible binding of one aromatic moiety and the *m*-xylylene bridge in the groove. A number of classical intercalators like mitoxantrone, diazaphenanthrene, quinacrine and adriamycin also show high affinities to polydA-polydT[4] with ΔT_m values between 13 and 23 °C, and almost all of them have cationic groups or side chains which give an additional groove binding contribution. Although the melting temperature of polydA-polydT is increased more efficiently by **7** than by any monofunctional compound, we still observe a lower affinity of **7** to polydA-polydT than to CT-DNA. From the thermal denaturation experiments, it seems that all the monofunctional compounds and **7** exhibit a preference for GC-rich sequences in CT-DNA, but UV- and fluorescence titrations of **1** and **6** with alternating polymers poly(dA-dT)$_2$ and poly(dG-dC)$_2$ (Table 3) gave rather similar binding constants to AT - as well as to GC - basepairs. For **6**, differences in calculated values of *n* and K_S between calf thymus DNA and alternating polymers (poly(dA-dT)$_2$ and poly(dG-dC)$_2$) are possibly due to conformational differences between these polymers.

Table 5 ΔT_m values (°C) of **1**, **6** and **7** with CT-DNA in *high* salt citric acid buffer pH = 5.0[a]

r	**1**	**6**	**7**
0.025	—	1.6[b]	1.3
0.05	0.7	3.8[b]	2.1
0.075	—	8.9	3.0
0.1	1.2	12.3	3.5
0.125	—	13.1	4.3
0.15	1.7	—	4.6
0.2	2.2	—	5.8
0.3	3.0	—	7.2
0.5	3.8	—	9.6

[a] See footnotes to Table 1, except: ionic strength $I = 0.12$ M. [b] Biphasic behaviour, the second transition could not be determined.

The ΔT_m value for **7** with the RNA-type polyA-polyU at the ratio of $r = 0.1$ is comparable with that of **1** at $r = 0.15$ (both with respect to stabilisation and destabilisation; see also Table 4), followed by a levelling off for the values at higher ratios than 0.1 to *ca.* −4.0/*ca.* +8.0 due to saturation. Compound **7** does not show a RNA selectivity anymore, the values for polydA-polydT are larger than for polyA-polyU.

Both the K_S and *n* obtained from Scatchard analysis (Fig. 2) of the bi-functional diazapyrenium derivatives **6** and **7** with CT-DNA show striking differences: K_S and *n* for **7** with *m*-xylylene bridge are in the range observed for the monofunctional diazapyrenium derivatives **1**, **2**, **4** and ethidium bromide, with K_S for **7** being around five and three times that of monofunctional **1** and **2**, respectively. However for **6** with *p*-xylylene bridge, K_S is more than 50 times larger than K_S exhibited by monofunctional **2** and close to two orders of magnitude larger than that of monofunctional **1**. These results, together with the fact that the ligand to nucleotide ratio *n* of 0.08 is well below the range characteristic for monointercalators suggest bisintercalation of **6** to CT-DNA.

On the other hand, viscometry (Fig. 3) shows a slope close to $\alpha = 1.0$ for **7**, which is even a little lower than that for the monomeric analogue **1** ($\alpha = 1.1$); also **6** does not exhibit much different behaviour ($\alpha = 1.12$). As a reference, ethidium bromide gives a slope of $\alpha = 1.0$ in this buffer as well as in PIPES10 buffer.[4] The viscosity results agree with the behaviour of bifunctional 9-aminoacridine compounds linked *via* the amino nitrogens by methylene chains of various length.[24] Four methylene

Table 6 NMR shift differences $\Delta\delta$ (ppm)[a] and peak halfwidth increases $W_{1/2}$ (Hz)[b] at various ligand/DNA phosphate ratios r[c]

		$r = 1.7$		$r = 0.86$		$r = 0.57$	
		$\Delta\delta$	$W_{1/2}$	$\Delta\delta$	$W_{1/2}$	$\Delta\delta$	$W_{1/2}$
4	H3/H8	−0.003	10	−0.010	18	−0.025	33
	H2/H7, H1/H6	+0.001	6	−0.007	18	−0.010	32
	Phenyl-H	+0.010	3	±0.00	16	−0.015	27
		±0.00		−0.006		−0.017	
3	H5/H10	−0.008	11	−0.010	36		
	H3/H8, H1/H6	−0.012	13	−0.023	18		
	H2/H7	−0.017	9	−0.026			
1 pH = 5.0	H5	−0.053	39		33		
	H10	−0.034	62				
	H1/H6, H3/H8	−0.076	63				
	H2/H7	−0.079	44				
1 pH = 7.0	H5	−0.053	29				
	H10	−0.0995	30				
	H1/H6, H3/H8	−0.104	63				
	H2/H7	−0.133	58				

[a] $\Delta\delta$ error ±0.001 for $W_{1/2} < 30$ Hz; ±0.004 for $W_{1/2} > 30$ Hz; unless noted otherwise. [b] $W_{1/2}$ error ±5 Hz, unless noted otherwise. [c] Measuring conditions: 298 K; $I = 0.04$ M, c(drug) = 1 mM.

groups together with the two nitrogens attached to the acridine ring are not sufficient in length to allow bisintercalation even if only one base pair is included in the intercalation site ("one base pair sandwich" model). The same can be assumed with **6** linked by a *p*-xylylene unit which is close in length to a hexamethylene bridge or a tetramethylene bridge containing two nitrogens, respectively. Drugs which are known to act as bisintercalators usually possess longer linkers.[25] The viscometry results would suggest rather monointercalation also with **6**, with binding of the second aromatic unit in the groove, but do not entirely rule out bisintercalation.

The thermal denaturation curves for the bifunctional ligand **6** in low salt citric acid buffer are completely different from the curves with all other compounds (see for example Fig. 1c) examined here: upon addition of **6** the first transition from ds- to ss-nucleic acid becomes shallower and flatter, with a decreasing absorbance, and the final step of the curve becomes continuously steeper and larger in absorbance (Fig. 1a). With increasing ligand to DNA-phosphate ratio the two regions merge resulting in one transition at temperatures above 90 °C. At ratios $r > 0.1$, one cannot determine even by graphical methods a midpoint of the curves with CT-DNA. Therefore the reported numbers for **6** with CT-DNA (Table 4) rely basically on the first transition. The values with **6** for the first step lie more or less in the same range, like those of the first transitions of the biphasic curves of **7** (for $r = 0.025$ and 0.05), and 4 to 7 °C lower than the melting point differences of the monophasic curves of **7** at the respective ratios of $r \geqslant 0.075$. The same behaviour can be seen in DMSO-containing low salt citric acid buffer which was applied in order to obtain a complete melting curve: all ΔT_m values were, as expected, lower, but again it was not possible to reach the final part of the CT-DNA curves of **6**. The melting increases for the first denaturation step of **7** are still in the same range as **6** at all measured ratios.

An inverse effect and more evaluable curves could be obtained in high salt citric acid buffer: at $r = 0.075$ and higher, there is only one broad melting step, comparable to curves with **7** (Fig. 1c). At $r < 0.075$, the biphasic behaviour could be due to an insufficient saturation of the nucleic acid by **6**. For the monophasic curves, the values for **6** are about three times larger than those for **7**, and 5 to 10 times larger than the respective numbers for **1** (Table 5). In slight contrast, the binding constants to CT-DNA show, in comparison to the melting point results, a much more pronounced decrease of 100 : 5 : 1 for **6** *versus* **7** and **1**. However, viscosity data (see above) support the same binding mode for both compounds with one aromatic unit intercalating, and the other one binding in a groove. The higher ΔT_m values for **6** indicate a better binding with the ligand containing a *p*-xylylene bridge in comparison to the *meta*-disubstituted phenyl unit in the ligand.

The melting curves of the polydA-polydT with **6** (Table 4; Fig. 1d) show a biphasic behaviour for $r < 0.15$, however, the low melting temperature of polydA-polydT itself (~47 °C) here allowed determination of the second transitions. For $r > 0.15$, the curves become monophasic with only the second melting step. A comparison of the values for $r = 0.2$ (34.1 °C) and $r = 0.3$ (37.6 °C) with the respective ones of **7** gives an increase of more than ~20 °C in the stabilisation of polydA-polydT by **6** compared to **7**. Also the biphasic curves for $r < 0.15$ show in both transitions larger ΔT_m values for **6** than for **7**. The first step ΔT_m values for **6** with polydA-polydT are comparable with, or even higher than those of the same compound with CT-DNA.

For polyA-polyU, there are already high values for both stabilisation and destabilisation at low $r < 0.025$. The fast saturation of polyA-polyU with **6** is consistent with the number n of bound ligand to CT-DNA phosphates obtained by Scatchard analysis (Table 3) which is half as large for **6** ($n = 0.07$) as for **7** ($n = 0.14$).

NMR titrations with CT-DNA could be performed with **1**, **3** and **4** (the last at different pH values), but due to solubility problems not with the bifunctional compounds **6** and **7**. At the chosen measuring concentrations, **3** and **4** showed no evidence of self-association in the concentration range between 1×10^{-4} and 1×10^{-2} M, indicated by the small shift changes < 0.003 ppm. This is in line with the reported weak self-association constant of ethidium bromide of about 400 l mol^{-1}.[26] In contrast, **1** exhibited strong downfield shifts of up to 0.04–0.1 ppm upon dilution. Unfortunately, no limiting shifts for the monomer and the dimer could be derived from dilution experiments as the concentration range was limited to the observation of linear parts due to sensitivity and solubility problems. Already at a ligand–DNA phosphate ratio of $r = 1.7$ (with the ligand still in excess), **1** shows upfield shifts of −0.03 up to −0.08 ppm at pH = 5.0, and concomitant large line broadenings of 40 to 70 Hz, clearly indicating intercalation of the aromatic units between the nucleobase pairs (Table 6, Fig. 4). At pH = 7.0, **1** gives larger upfield shifts (−0.053 to −0.133 ppm). In the case of **3**, the upfield shifts and line broadenings at $r = 1.7$ are less pronounced (−0.01 till −0.02 ppm; ~10 Hz), but with DNA phosphate in excess ($r = 0.86$) a line broadening typical for intercalation of 18–36 Hz is observed; the upfield shifts still remain quite low compared with **1**. For **4** the shift changes at $r = 1.7$ and $r = 0.86$ are comparable with those of a groove binder: small upfield and downfield shifts < ±0.01 ppm.

However, at $r = 0.86$ the line broadenings are close to the values typical for intercalation (16 to 18 Hz). At a higher DNA phosphate excess ($r = 0.57$), the line broadening increases to up to 33 Hz with upfield shifts of up to −0.025 ppm. The absence of larger upfield shifts can be due to fast exchange between protons more or less exposed to the nucleobase shielding cones and their deshielding edges. Distinct line width increases are, however, a more reliable indicator of intercalation, even in the absence of larger shielding effects.

Experimental

Solutions

Low salt citric acid buffer contained 0.01 M citric acid adjusted to pH = 5.0, high salt citric acid buffer contained 0.0243 M citric acid and 0.0514 M Na_2HPO_4 (pH = 5.0); for pH = 4.5, 0.0273 M citric acid and 0.0455 M Na_2HPO_4, respectively. The phosphate buffers used for NMR measurements contained 0.02 M Na_2HPO_4 in D_2O, adjusted to pH = 7.0 (pD = 7.4) or pH = 5.0 (pD = 5.4), respectively.

For the melting and viscometry experiments calf thymus (CT)-DNA (Aldrich) was dissolved in low salt citric acid buffer (for NMR, phosphate buffer), sonicated and filtered through a 0.45 μm filter. PolydA-polydT and polyA-polyU (both from Sigma) were dissolved in the buffer. The phosphate concentrations were determined spectrophotometrically at $\lambda = 260$ nm by using $\varepsilon = 6600$ l mol^{-1} cm^{-1} for CT-DNA and 6000 l mol^{-1} cm^{-1} for the polymers.

UV and fluorescence titrations

These were performed at room temperature in aqueous buffer (citric acid–Na_2HPO_4, pH 4.5) at constant ionic strength ($I = 0.1$ M). Aliquots of DNA solutions were successively added to the solution of the respective 4,9-diazapyrenium or phenanthridinium derivative at $1–5 \times 10^{-6}$ M concentration and fluorescence or UV spectra recorded. After corrections for dilution, the titration data were processed according to Scatchard equation by nonlinear fitting, assuming the binding sites for intercalation as the concentration of the substrate. To exclude the possible inner filter effects at high nucleic acid concentration the excitation wavelengths used in fluorimetric titrations were higher than 350 nm. As checked by UV, in this range no nucleic acid absorptions at their highest concentrations used in fluorimetric titrations could be observed. Measurements with **3** and **5** were hampered by lack of stability in the absence of DNA.

Thermal melting curves

These were obtained with a Cary 1 Bio UV/Vis-spectrophotometer (Varian) connected with a temperature-controller (Varian) and interfaced to a PC. A thermistor fixed into a reference cuvette was used to monitor the temperature. The nucleic acid was added to 1 ml of buffer in quartz semi-microcuvettes of 1 cm path length, and the concentration was determined by measuring the absorbance at 260 nm. Experimental concentrations for CT-DNA were *ca.* 8×10^{-5} mol l^{-1}, for polydA-polydT and polyA-polyU *ca.* 4×10^{-5} mol l^{-1}. The melting curves were recorded at different compound-to-nucleic acid phosphate-ratios (r) by following the absorption change at 260 nm as a function of temperature with a heating rate of 0.5 °C min^{-1}. The absorbance of the ligands, and their absorbance change with temperature were subtracted from every curve, and the absorbance scale was normalized. T_m values are the midpoints of the transition curves, determined from the maximum of the first derivative or graphically by a tangent method[27] (in cases where a complete melting profile could not be obtained, as with ligand **6** and CT-DNA, the final tangent was drawn through the increasing final part of the curves). ΔT_m values were calculated subtracting T_m of the free nucleic acid from T_m of complex. Every ΔT_m value reported here was the average of at least two measurements, the error in ΔT_m is ±0.5 °C.

Viscometry measurements

These were conducted with an automatic Ubbelohde micro viscometer system AVS 350 (Schott) connected to a PC. The temperature was maintained at 25 ± 0.05 °C with a Schott thermostat CT 1450. Aliquots of drug stock solutions were added to 3.2 ml of 5×10^{-4} M CT-DNA solution in low salt citric acid buffer, with a compound to DNA phosphate ratio r less than 0.15. Dilution never exceeded 4% and was corrected for in the calculations. The flow times were measured at least five times optically by light barrier with a deviation of ±0.02 s. The viscosity index α was obtained from the flow times at varying r according to eqn. (1),[28] where T_0, t_{DNA} and t_r denote the flow times of buffer, free DNA and DNA complex at reagent/phosphate ratio r, respectively; L/L_0 is the relative DNA lengthening. The L/L_0 to r-plot was fitted to a straight line that gave slope α. The error in α is ±0.1.

$$L/L_0 = [(t_r - t_0)/(t_{DNA} - t_0)]^{1/3} = 1 + \alpha r \qquad (1)$$

NMR Spectra

These were obtained with a Bruker AM 400 spectrometer at 25 °C with a drug concentration of 1 mM; the number of scans was about 500. Titrations were conducted adding aliquots of CT-DNA (in 20 mM phosphate buffer) to 0.5 ml of drug solution over a range of drug–DNA phosphate ratios of 1.7 to 0.57. Samples were referenced to TMS as an external standard. Data were processed either on the spectrometer or on a PC with the program WIN-NMR (Bruker); the line broadening was set to 15 Hz in all spectra to improve the signal-to-noise ratio. The line broadening increase was determined subtracting the width of the signals at half height in the spectrum without DNA from those in the spectra with DNA. Errors are given in the footnotes of Table 6.

Acknowledgements

The work in Saarbrücken is supported by the Deutsche Forschungsgemeinschaft, Bonn, and the Fonds der Chemischen Industrie, Frankfurt. Additional support by the Osteuropa Büro of the German BMBF is also acknowledged.

References

1 (*a*) W. Saenger, *Principles of Nucleic Acid Structure*, Springer, New York, 1988; (*b*) W. D. Wilson, in *Nucleic Acids in Chemistry and Biology*, ed. M. Blackburn and M. Gait, IRL Press, Oxford, 1989, ch. 8; (*c*) J. W. Lown, *Anti-Cancer Drug Des.*, 1988, **3**, 25; (*d*) P. B. Dervan, *Science*, 1986, **232**, 464; (*e*) S. Neidle and T. C. Jenkins, *Molecular Design and Modeling, Part B*, 1991, **203**, 433; (*f*) D. S. Johnson and D. L. Boger, DNA Binding Agents, ch. 3, in *Comprehensive Supramolecular Chemistry*, vol. 4, series ed. J.-M. Lehn, vol. ed. Y. Murakami, Pergamon Press, Oxford, England, 1996, 73.

2 (*a*) see P. Hobza, J. Sponer and M. Polasek, *J. Am. Chem. Soc.*, 1995, **117**, 792; J. Sponer, J. Lesczynski and P. Hobza, *J. Phys. Chem.*, 1996, **100**, 5590; (*b*) J. Sponer and P. Hobza, *Int. J. Quant. Chem.*, 1996, **57**, 959; (*c*) J. Sponer, J. Lesczynski, V. Vetter and P. Hobza, *J. Biomol. Struct. Dyn.*, 1996, **13**, 695; (*d*) R. A. Friedmann and B. Honig, *Biopolymers*, 1992, **32**, 145; (*e*) P. Hobza, M. Kabelaz, J. Sponer, P. Meijzlik and J. Vandrasek, *J. Comput. Chem.*, 1997, **18**, 113; (*f*) H.-J. Schneider and J. Sartorius, in *Physical Supramolecular Chemistry*, eds. L. Echegoen and A. E. Kaifer, (NATO ASI Ser. C) 1996, p. 11; and references cited therein.

3 References on RNA interactions with small ligands, see (*a*) Li Ke, M. Fernandez-Saiz, C. T. Rigl, A. Kumar, K. G. Ragunathan, A. W. C. McConnaughie, D. W. Boykin, H.-J. Schneider and W. D. Wilson, in *Bioorganic and Medicinal Chemistry; Symposium Issue "Strategies for RNA Recognition"*, ed. S. Hecht, 1997; D. W. Wilson, Y. Li and J. Veal, in *Advances in DNA Sequence Specific Agents*, vol. 1, p. 89; ed. L. H. Hurley, JAI Press, Inc., Greenwich, 1992.

4 W. D. Wilson, L. Ratmeyer, M. Zhao, L. Strekowski and D. Boykin, *Biochemistry*, 1993, **32**, 4098.
5 I. Piantanida, V. Tomišič and M. Žinič, *J. Chem. Soc.*, *Perkin Trans. 2*, 2000, preceding article.
6 (*a*) L. Strekowski, J. L. Mokrosz, W. D. Wilson, M. J. Mokrosz and A. Strekowski, *Biochemistry*, 1992, **31**, 10802; (*b*) A. J. Hopfinger, M. G. Cardozo and Y. Kawakami, *J. Chem. Soc.*, *Faraday Trans.*, 1995, **91**, 2515; (*c*) H.-J. Schneider and J. Sartorius, *J. Chem. Soc.*, *Perkin Trans. 2*, 1997, 2319 and references cited therein.
7 J. Blacker, J. Jazwinski and J.-M. Lehn, *Helv. Chim. Acta*, 1987, **70**, 1; J. Blacker, J. Jazwinski, J.-M. Lehn and F. X. Wilhelm, *J. Chem. Soc.*, *Chem. Commun.*, 1986, 1035; A. Slama-Schwok, J. Jazwinski, A. Bere, T. Montenay-Garestier, M. Rougée, C. Hélène and J.-M. Lehn, *Biochemistry*, 1989, **8**, 3227; A. Slama-Schwok, M. Rougée, V. Ibanez, N. E. Geacintov, T. Montenay-Garestier, J.-M. Lehn and C. Hélène, *Biochemistry*, 1989, **8**, 3234.
8 A. M. Brun and A. Harriman, *J. Am. Chem. Soc.*, 1991, **113**, 8153; C. Coudret and A. Harriman, *J. Chem. Soc.*, *Chem. Commun.*, 1992, 1755.
9 L. Kibler-Herzog, B. Kell, G. Zon, K. Shinozuka, S. Mizan and W. D. Wilson, *Nucleic Acids Res.*, 1990, **18**, 3545.
10 (*a*) C. R. Cantor and P. R. Schimmel, *Biophysical Chemistry*, Part III, W. H. Freeman and Co. 1980, p. 1233; (*b*) H. W. Zimmermann, *Angew. Chem.*, *Int. Ed. Engl.*, 1986, **25**, 115; (*c*) J. D. McGhee and P. H. von Hippel, 1974, **86**, 469 and 1976, **103**, 679.
11 S. Chandrasekaran, S. Kusuma, D. W. Boykin and W. D. Wilson, *Magn. Res. Chem.*, 1986, **24**, 630; J. Sartorius and H.-J. Schneider, *FEBS Lett.*, 1995, **374**, 387.
12 M. Wirth, O. Buchardt, T. Koch, P. E. Nielsen and B. Norden, *J. Am. Chem. Soc.*, 1988, **110**, 932.
13 S. F. Yen, E. J. Gabbay and W. D. Wilson, *Biochemistry*, 1982, **21**, 2070; W. D. Wilson and F. A. Tanious, in: *Molecular Aspects of Anticancer Drug–DNA Interactions*, ed. S. Neidle and M. J. Waring, Macmillan Press, Riverside, N.Y.; F. A. Tanious, S. F. Yen and W. D. Wilson, *Biochemistry*, 1991, **30**, 1813; W. Müller and D. M. Crothers, *J. Mol. Biol.*, 1968, **35**, 251; J. A. Elliot, W. D. Wilson, R. G. Shea, J. A. Hartley, K. Reszka and J. W. Lown, *Anti-cancer Drug Design*, 1989, **3**, 271.
14 Ref. 10, p. 1137–44; C. L. Stevens and G. Felsenfeld, *Biopolymers*, 1964, **2**, 293.
15 R. Lauceri, T. Campagna, A. Contino and R. Purrello, *Angew. Chem.*, *Int. Ed. Engl.*, 1996, **35**, 215.
16 J. M. Waring, *Biochem. J.*, 1974, **143**, 483.
17 J. Mergny, D. Collier, M. Rougée, T. Montenay-Garestier and C. Hélène, *Nucleic Acids Res.*, 1991, **19**, 1521; N. T. Thuong and C. Hélène, *Angew. Chem.*, *Int. Ed. Engl.*, 1993, **32**, 666.
18 D. S. Pilch and K. J. Breslauer, *Proc. Natl. Acad. Sci. USA*, 1994, **91**, 9332.
19 Ref. 1(*a*), p. 305.
20 Ref. 10(*a*), p. 1144.
21 Ref. 10(*a*), p. 1135.
22 A. Czarny, D. W. Boykin, A. A. Wood, C. M. Nunn, S. Neidle, M. Zhao and W. D. Wilson, *J. Am. Chem. Soc.*, 1995, **117**, 4716.
23 D. L. Boger and D. S. Johnson, *Angew. Chem.*, *Int. Ed. Engl.*, 1996, **108**, 1438 and references herein; D. L. Boger and D. S. Johnson, *Proc. Natl. Acad. Sci. USA*, 1995, **92**, 3642.
24 L. P. G. Wakelin, M. Romanos, T. K. Chen, D. Glaubiger, E. S. Canellakis and W. J. Waring, *Biochemistry*, 1978, **17**, 5057; L. P. G. Wakelin, *Med. Res. Rev.*, 1986, **6**, 273 and references herein.
25 M. Cory, D. D. McKee, J. Kagan, D. W. Henry and J. A. Miller, *J. Am. Chem. Soc.*, 1985, **107**, 2528; S. C. Zimmerman, C. R. Lamberson, M. Cory and T. A. Fairley, *J. Am. Chem. Soc.*, 1989, **111**, 6805; J. M. Veal, Y. Li, S. C. Zimmerman, C. R. Lamberson, M. Cory, G. Zon and W. D. Wilson, *Biochemistry*, 1990, **29**, 10918.
26 D. B. Davies, L. N. Djimant and A. N. Veselkov, *J. Chem. Soc.*, *Faraday Trans.*, 1996, **92**(**3**), 383.
27 W. D. Wilson, F. A. Tanious, M. Fernandez-Saiz and C. T. Rigl, Evaluation of Drug/Nucleic acid Interactions by Thermal Melting Curve, from: *Methods in Molecular Biology*, *Vol. 90: Drug-DNA Interaction Protocols*, ed. K. R. Fox, Humana Press Inc., Totowa, N.Y.
28 G. Cohen and H. Eisenberg, *Biopolymers*, 1969, **8**, 45; M. Wirth, O. Buchardt, T. Koch, P. E. Nielsen and B. Nordén, *J. Am. Chem. Soc.*, 1988, **110**, 932.

Paper a905307g